Journal of Visualization, Vol. 4, No. 4 (2001) 341-348

Visualization Study on the Layer Formation of Electro-rheological Fluid

Okamoto, K.*, Nakatsukasa, T.* and Madarame, H.*

* Nuclear Engineering Research Laboratory, The University of Tokyo, Tokai-mura, Ibaraki, 319-1188, Japan.

Received 22 June 2001.
Revised 7 September 2001.

***Abstract*:** The visualization study on the microstructure of the Electro-Rheological (ER) fluid was carried out. The dense particle motion was difficult to visualize because of the severe light scattering by the particle itself. In this study, the laser light sheet was illuminated to visualize the dense particle condition, 10 wt%. As the ER fluid, the cholesterol particles (~20 μm) were dispersed into the silicone oil (10 cS). The humidity of particle was controlled to be 4%. The particle density was set to be 10 wt%. Under this condition, individual particle could not be distinguished. However, the particle cluster motion could be clearly visualized. With the electrical field, the chains of the particles were formed. The ER fluid with the chain was recorded onto the video camera. With higher electrical field, the layer of the particle was formed at the top and bottom electrode. The layer caused the decrease of the fluid channel width, resulting in the resistance to be increased. The effects of electrical field on the layer formation were experimentally investigated. The Mason number, which is the ratio of shear force to electrical force, was found to be the key parameter of the layer formation.

***Keywords*:** electro-rheological fluid, layer formation, laser sheet, photochromic dye

1. Introduction

An electro-rheological (ER) fluid is a suspension fluid of solid particles in a dielectric oil which shows a reversible increase of apparent viscosity by an electric field applied (Halsey, 1992). This phenomenon is called ER effect. Applying an electric field to the ER fluid, particles in oil are induced polarization, resulting in the attraction between particles. Then the chain structure of particles connecting both electrodes has been formed. This chaining is one of the important characteristics in the ER effect. The ER fluids can be approximately described as a Bingham fluid.

Due to the capabilities to control the apparent viscosity, the ER fluids are tried to apply in clutches, valves, shock absorber and pumps (Wong et al., 1993). Many researches on ER fluid have been carried out both experimentally and theoretically. The ER effects for the pressure drop have been investigated in two parallel electrodes, where the flow established the Poiseuille-flow (Zukoski et al., 1986). The shear stress and the yield stress have been investigated using the rheometer (Nakano et al., 1996).

The mechanisms of ER effects have not been clarified yet completely. In order to discuss the mechanisms, the particle behavior in the fluids should be investigated. Tsukiji et al. (Tsukiji et al., 1997; Tsukiji et al., 1999) visualized the particle behavior in two parallel electrodes. The conditions of the particle concentration were from 0.04 wt% to 20 wt%. Since the dense concentration causes the severe light scatter, it is easy to visualize the particle behavior in the lower concentration field. However, as higher concentration is usually required, it is important to visualize the particle behavior in the higher particle concentration.

In this study, the electro-rheorogical characteristics of the higher concentration fluid were evaluated with visualization. The laser light sheet technique and photochromic dye activation method were applied to visualize the ER fluid.

2. Experiment

The experimental setup is schematically shown in Fig. 1. The test section was a rectangular channel with two parallel electrodes, top and bottom. The cross section of the channel was 10 mm in height, 5 mm in width and 300 mm in length. The length of the electrodes was 100 mm, which was installed at the center of the channel. High voltage was applied to the electrodes in the range of 0 - 1.5 kV/mm by the high voltage power supply (Glassman high voltage-MJ15P1000-10). The vertical wall was made of transparent acrylic resin. The top and bottom electrodes were made of ITO-glass. Since the ITO-glass is transparent for the light of ultra violet to infrared, the laser can be introduced through the electrode. Thus the flow in the channel could be visualized clearly.

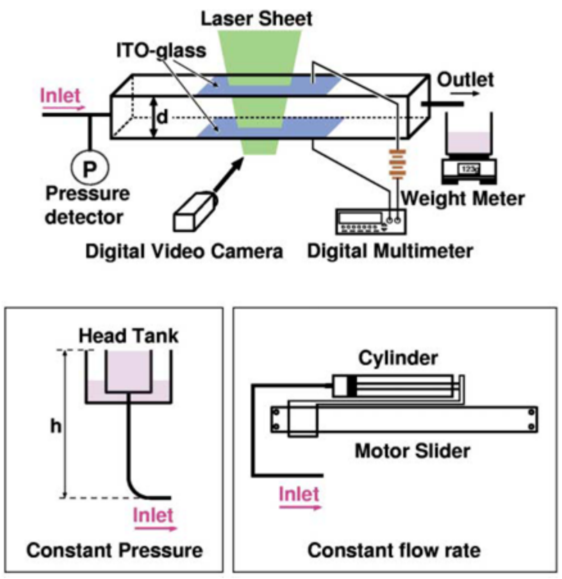

Fig. 1. Experimental setup.

As an ER fluid, a mixture of silicone oil (Shin-etsu, KF96) and micro-cristalized cellulose (Asahi Chemical, PM-M25) was used. The diameter of the cellulose is about 25 ㎛. The concentration of the particle is 10 wt% and the kinetic viscosity of the silicon oil was 100 cS. The water concentration ratio in the cellulose was controlled to be about 4%, because the ER effects depended on the water ratio in the particle.

Two kinds of flow supply system were applied to the above test section. One was constant pressure system (P), and the other was constant flow rate system (F).

In the constant pressure system (P), the constant pressure was applied to the test section using a head tank. The mass flow rate was measured by the electric weight meter at the outlet. Initially, the ER fluid flowed without electric field. At $t = 0$, the electric field (E) was applied between the top and bottom ITO electrodes. The laser light sheet illuminated the channel through the ITO glass. Since the concentration ratio of the particle was relatively large, 10 wt%, illuminated laser light was scattered by the particles. Therefore, the illumination was not the plane light, however, the particle structures inside the ER fluid could be clearly visualized. The images of the fluid flow between the electrodes were recorded onto the digital video camera (Sony-DCR-VX1000). The flow rate variation and the visualized images were simultaneously recorded.

In the constant flow rate system (F), the ER fluid was pushed by the computer controlled piston. Varying the piston velocity, the flow rate could be controlled. The pressure at the upstream of the test section was measured by pressure gauge. Also, the visualized ER fluid was recorded simultaneously.

At the test section, the electric field strength was applied between the top and bottom ITO electrodes. In the (P) system, flow rate was measured with constant pressure. While, the pressure was measured with constant flow rate in the (F) system.

3. Experimental Results

3.1 Constant Pressure (P) System

Using the head tank, the constant pressure was applied to the test section. The head was set to be 100, 200 and 400 mm.

Figure 2 shows the variation of the flow rate under the condition of h = 200 mm. Several experiments for a certain condition were carried out to check the reproducibility. Since the reproducibility was fairly well, the typical data were plotted on the figures. At t = 0, just after the electricity application, the flow rate quickly decreased. When E = 0.1 - 0.7 kV/mm, the flow rate continuously decreased, then converged to a certain value. When E = 0.8 - 1.0 kV/mm, the flow rate decreased more rapidly, however, it fluctuated after several seconds. The amplitude of the flow rate fluctuation depended on the electric field strength, E. When E exceeded 1.1 kV/mm, the flow rate finally decreased to zero, i.e., the flow passage was plugged. The plugged phenomena was called as "Chain Stuck." The variation of the flow rate depended on the electric field strength. The similar tendency was observed under the other pressure conditions (h = 100, 400 mm).

The visualized particle behavior in the channel was simultaneously recorded. Figure 3 shows the example of the visualized images. Under E = 0.7 kV/mm, the dispersed particles connected with forming the chain structure.

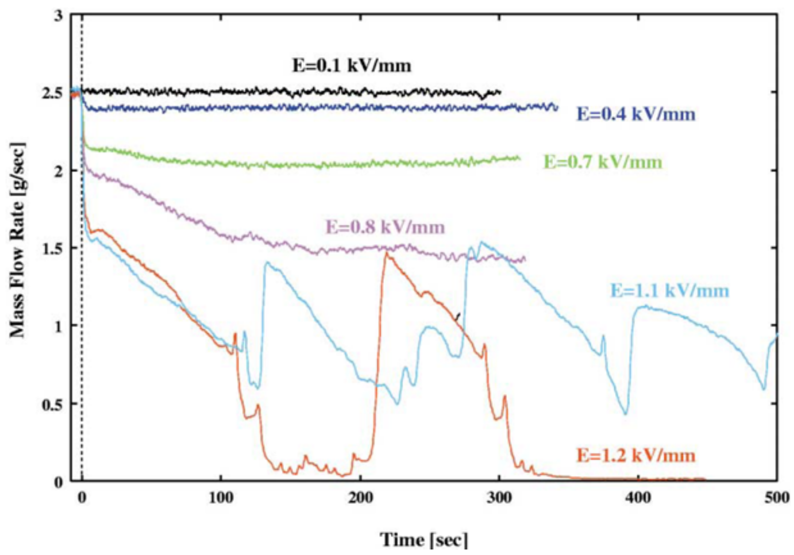

Fig. 2. Mass flow rate for constant pressure case (h = 200 mm).

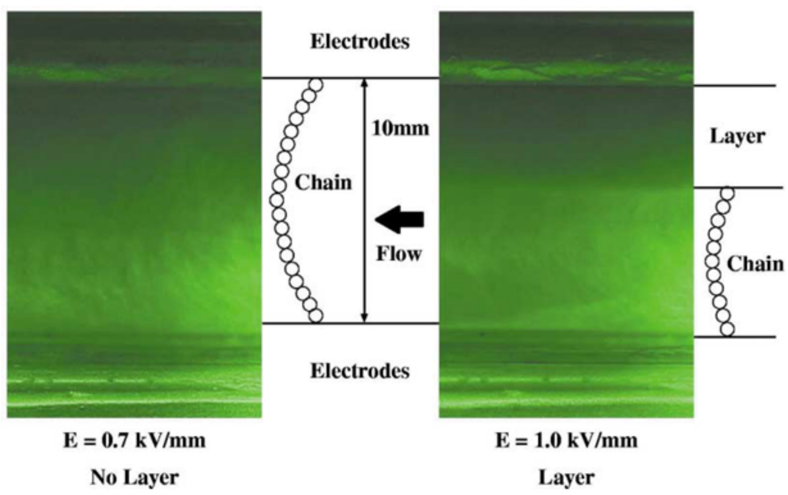

Fig. 3. Visualized images for constant pressure case (h = 200 mm).

The chain structure was curved to be an arrow shape because of the fluid force. Keeping the arrow shape, the chain flowed downstream. This arrow shape structure caused the fluid resistance, i.e., ER effects, resulting in the reduced flow rate as shown in Fig. 2. Under higher electric field strength E = 1.0 kV/mm, thicker chains were formed. Also, the particle layer was formed close to the top electrode. The chain flowed downstream through the gap between the top layer and bottom electrode. Some chains might break, then they stuck onto the layer forming the layer to be thicker. The thickness of the layer grew with time, causing the resistance of the channel to increase. Sometimes, the layer was cleaned away by the fluid force, then the layer was forming again, resulting in the fluctuation of the flow rate as shown in Fig. 2.

3.2 Constant Flow Rate (F) System

The constant flow rate Q was applied to the test section. The average inlet velocity, u, is varied from 0.02 to 0.2 m/s. Figure 4 shows the variation of the pressure with time for the different electric fields at the constant flow rate of 0.02 m/s. Initially, the fluid flowed constantly without electric field. At t = 0, a certain electric field was applied to the electrodes. With applying the electric field, the pressure rapidly increased to a certain value. Then the pressure was almost constant at E = 0.1 - 0.5 kV/mm as shown in Fig. 4. With increasing the electric field, the pressure also increased. When E exceeded 0.6 kV/mm, the pressure increased monotonously, following the fluctuation. The pressure increasing ratio also depended on the electric field. The similar tendency was observed for the other flow rate cases.

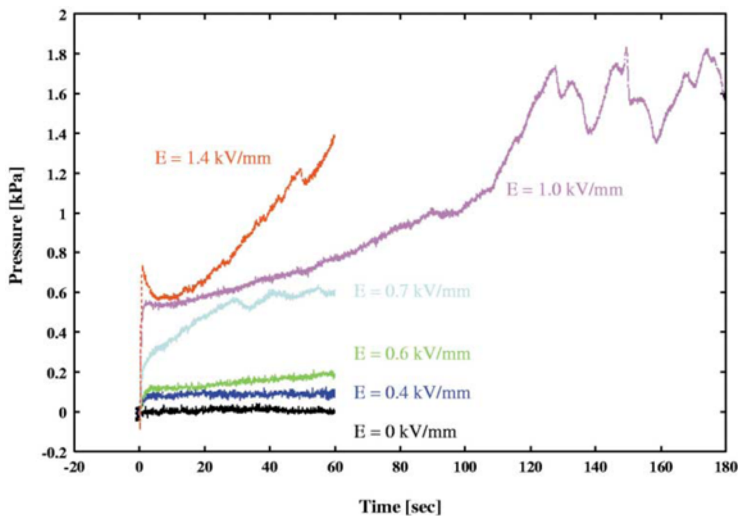

Fig. 4. Pressure for constant flow rate case (u = 0.02 m/sec).

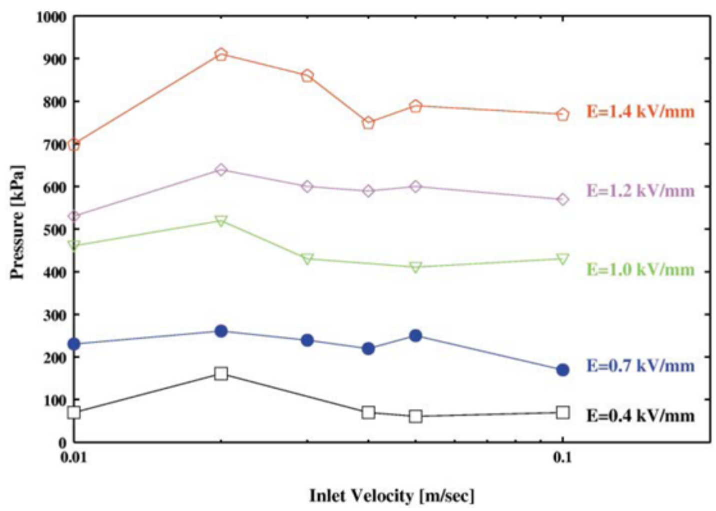

Fig. 5. Relation between inlet velocity and pressure at constant flow rate.

Figure 5 summarizes the relationship between the flow rate and pressure. Because the pressure increases with time for higher electric field, the pressure just after the electricity application was taken. This pressure was considered to show the ER effects. The pressure, i.e., the resistance, is independent of the flow rate, however, it depends on the electric fields. The tendency of the present results is almost the same as Tsukiji's experimental results (Tsukiji et al., 1997), indicating the present ER fluids to be the normal ER fluids. The pressure in Fig. 5 was found to be proportional to the square of the electric field (E^2). This result indicates that the pressure just after the electricity application was caused by the strength of the particle chain structure (E^2).

The particle layer was visualized under the constant flow rate experiment. Local concentration of the particle might be increased in the chain structures. When the concentration exceeded a certain limit, the chain was broken with forming the layer on the wall. Since there was huge shear close to the wall, the particles moved to the wall, forming the wall. The layer formation and break were also observed, causing the pressure fluctuation in Fig. 4.

3.3 Layer Formation

The flow characteristics were investigated for the constant pressure (P) and constant flow rate (F) cases, using the visualized images, the variation of flow rate (Fig. 2) and pressure variation (Fig. 4). The flow conditions were classified into two conditions.

1. Conversion to steady flow without forming Layer
2. Fluctuating flow with forming Layer (including chain stuck)

To evaluate the flow, the non-dimensional variable, Mason number (Mn) was introduced. Mason number is expressed as the ratio between the shear forces and polarization forces

$$Mn = \frac{h_0 \dot{g}}{2e(bE)^2} \qquad (1)$$

where, e is the permittives of oil phase, b is the function of permittives of both the particles and oil, h_0 is viscosity, $\dot{g}$ is the shear rate. Since the shear rate could not be measured in this study, the viscous force was assumed to be proportional to the shear force. With above assumption, Mn could be expressed as follows,

$$Mn = \frac{nu}{e_0 \, r b E^2} \qquad (2)$$

where, b, u, e_0, n and r denote the channel height, the average velocity, permittives in vacuum kinetic viscosity and density, respectively. Figure 6 shows the summary of the Layer formation condition with a function of Mn and Re. Reynolds number (Re) was defined as,

$$Re = \frac{2uab}{n(a+b)} \qquad (3)$$

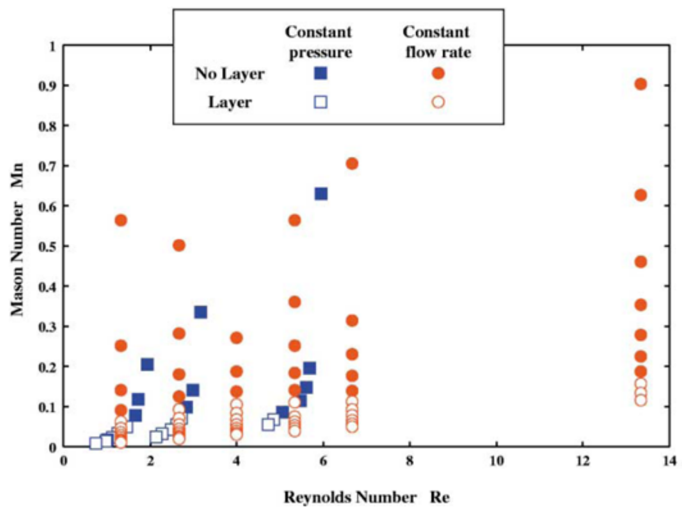

Fig. 6. Layer formation condition (Mn - Re).

where *a* and *b* denote the width and height of the channel. Open mark denotes the layer formation condition. The Box and Circle denote the constant pressure (P) and constant flow rate (F) cases, respectively. The layer could be formed under lower *Mn* condition. In this experiment, the limit *Mn* was about 0.1. The fluid velocity (u) and square of electric field strength (E^2) related to the layer formation.

3.4 Velocity Measurement by Photochromic Dye

The mechanism of the layer formation was related to the velocity distributions of the ER fluid. The visualized images just show the movement of particle chain. The resistance was considered to be caused by the interaction between the chain motion and fluid motion. The small particle and the fluid flow might have the relative velocity, (slip velocity). However, no data have been reported for the fluid and particle chain velocities, under high concentration of particles. Because of the dense particle condition, the particle movement could not be measured. The particle chain motion was qualitatively visualized by laser sheet as mentioned in the previous section.

In this study, the flow field inside the ER fluid was visualized, using the Photochromic dye. The dye was dissolved into silicon oil. Only the flow of the silicon oil could be visualized. The particles were not visualized. The dye was 1,3,3,-Trimethylindolino-6'-nitrobenzopyrylospiran with the concentration of 0.05 wt%. Usually, the dye was transparent. With absorption of the ultraviolet laser light, the dye was photochromized with the violet color. The photochromism was activated for several seconds. The fluid illuminated by the ultraviolet light was treated as the tracer.

The fluid was illuminated by the pulse laser (Nd:YAG, 355 nm) whose pulse duration was about 10 ns. The

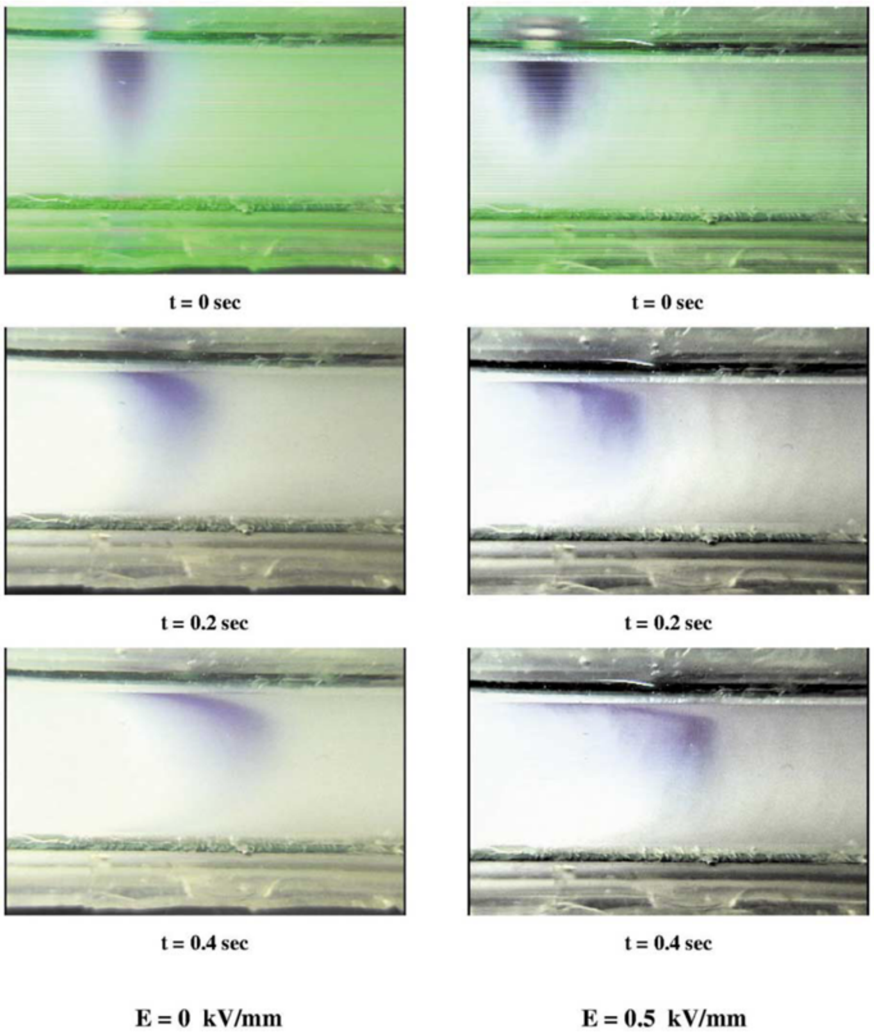

Fig. 7. Visualized images by photochromic dye.

diameter of the laser was about 1 mm so that only the line along the laser was photochromized. The laser was introduced from the top of the channel at $t = 0$.

Figure 7 shows the example of the visualized images for every $t = 0.2$ sec, under the condition of the average velocity $u = 0.02$ m/s. The electric fields were $E = 0$ and 0.5 kV/mm, respectively. The fluid was photochromized along the laser passage at $t = 0$. Because of the light scatter by the dense particles, the laser light diffused at the top area. The concentration ratio of the particle was too dense to generate the thin laser pass line. Also, the laser did not reach to the bottom wall because of the scattering and absorption. Only the top half area was visualized by this technique. The colorized fluid flowed downstream with time. The line indicated the velocity distribution of the ER fluid. The fluid velocity characteristics were completely different with and without electric filed ($E = 0$ and 0.5 kV/mm).

To quantize the velocity distribution, the captured images were processed with digital analysis. Because of the scatter, the line width was relatively large. Using the image processing technique, the center of the photochromized line was extracted. Figure 8 shows the extracted lines which denote the velocity distributions. Without the electric field ($E = 0$ kV/mm), the ER fluid flowed with Hagen-Poiseuiller flow. While, with the electric field ($E = 0.5$ kV/mm), the shear close to the wall was very strong. The center area flowed with almost the same velocity. The plug flow was formed clearly. The large shear may cause the particle chain break, resulting in the layer formation.

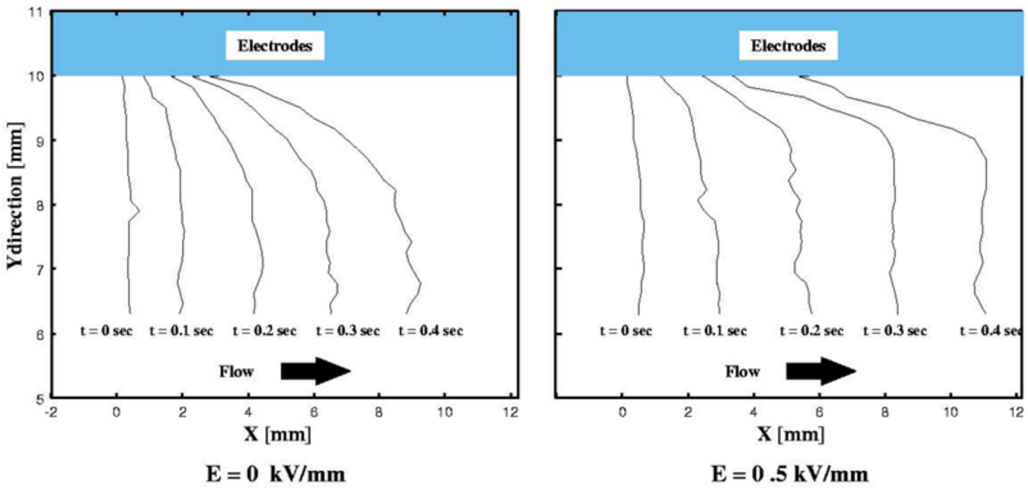

Fig. 8. Velocity distribution.

4. Conclusion

Under lower Mason number (*Mn*) condition, the layer was formed between the electrodes. The layer formation affected the ER flow condition. The characteristics of the flow highly depended on the mean velocity (u) and electric force ($\propto E^2$).

Using the photochromic dye, the velocity distributions of the silicone oil in the ER fluids were visualized, under very high concentration of particles (10 wt%). The plug flow was clearly visualized in the ER fluid. The high shear close to the wall caused the particle chain break, resulting in the particle layer at the wall.

References

Halsey T. C., Electrorheological Fluids, Science, 258-5083, (1992), 761.

Nakano, M. and Yonekawa, T., Active Damper Using Electrorheological Suspension and its Application to Vibration Isolation Control, Trans. JSME, C62-593, (1996), 33, (in Japanese).

Tsukiji, T. and Utashiro, T., Flow of ER Fluids between Two Parallel-plate Electrodes for Sinusoidal Electric Fields ,Trans. JSME, B63-608, (1997), 1221 (in Japanese).

Tsukiji, T., Tsurumaki H., Asako, Y. and Kawakami, T., Pressure Drop and Cluster Formation of ER Suspensions, Proceedings of 3rd ASME/JSME Joint Fluid Engineering Conference, (1999), FEDSM99-7135.

Wong, J. Y., Wu, X. M., Sturk, M. and Bortolotto, C., On the Applications of Electro-rheological Fluids to the Development of Semi-active Suspension Systems for Ground Vehicles, CSME, 17-4B, (1993), 789.

Zukosuki, C. F. and Goodwin, J. W., Towards the Electrical Control of Viscosity, IECON'86, (1986).

Author Profile

Koji Okamoto: He received his M.Sc.(Eng.) in Nuclear Engineering in 1985 from The University of Tokyo. He also received his Ph.D. in Nuclear Engineering in 1992 from The University of Tokyo. He worked in Department of Nuclear Engineering, Texas A & M University as a visiting associate professor in 1994. He works in Nuclear Engineering Research Laboratory, The University of Tokyo as an associate professor since 1993. His research interests are quantitative visualization, PIV, holographic PIV flow induced vibration and thermal-hydraulics in nuclear power plant.

Takayuki Nakatsukasa: He received his M.Sc.(Eng.) in Nuclear Engineering in 2000 from The University of Tokyo. He works in Energy & Environment Technology Department, The Japan Research Institute, Ltd.. His works are mainly on calculations for thermal-hydraulics fluid dynamics in nuclear power plant.

Haruki Madarame: He received his master's degree in Mechanical Engineering in 1972 from The University of Tokyo. He worked at Toshiba Research and Development Center from 1972 to 1975. He got his doctor's degree in Mechanical Engineering in 1976, and began to work in Nuclear Engineering Department, The University of Tokyo as an associate professor. He has been a professor of the Nuclear Engineering Research Laboratory, the University of Tokyo since 1990. His current interests include thermal hydraulics, flow-induced oscillations and nuclear reactor safety.